Paper:

Adaptive Gait for a Leg-Wheel Robot Traversing Rough Terrain (Second Report: Step-Up Gait)

Shuro Nakajima and Eiji Nakano

The Department of Advanced Robotics, Chiba Institute of Technology
2-17-1 Tsudanuma, Narashino, Chiba 275-0016, Japan
E-mail: shuro.nakajima@it-chiba.ac.jp
[Received April 4, 2008; accepted April 4, 2008]

A leg-wheel robot with four legs and two wheels mechanically separated features high mobility and stability on rough terrain. The adaptive gait for such terrain consists of three gait strategies. Here we focus on a step-up gait, part of an adaptive gait. Simulation and experiments demonstrated the feasibility of our proposal.
Regarding the point of the step-up gait flow, when the robot reaches a step, it does not advance easily because it cannot take a normal gait in ascending the step.
The difference between actual and desired wheel angles grows. The starting point of the step is detected using this information. The robot stops and prepares to ascend the step, placing all legs at the starting points of their work space. The robot then rises supported by its legs and wheels to enhance stability and to reduce energy use. To rise, it requires (1) acquisition of the target rise and (2) the correspondence in the difference between targeted and actual height.[1]

Keywords: mobile robot, leg-wheel robot, adaptive gait strategy, large rough terrain

1. Introduction

Legs enabling robots to make arbitrary, irregular contact with the ground can stably traverse a wide range of terrain, including steps and slopes. Legs are mechanically complex, however, and positioning and leg control relies on environment recognition, making practical use difficult.

We have been studying separated leg-wheel robots with 4 legs, two in the front and two in the back, each having 3 degrees of freedom (DOF), and with 2 independent wheels, one on each side, to enable robots to traverse unknown rough terrain but requiring less precision in environment recognition and simpler control [1, 2] (**Fig. 1**). We propose basic movement control [1] for rough terrain uneven within ± 0.1 m, i.e., regular rough terrain, without the need for environment-recognition sensors. Basic movement control does not cover much more uneven terrain.

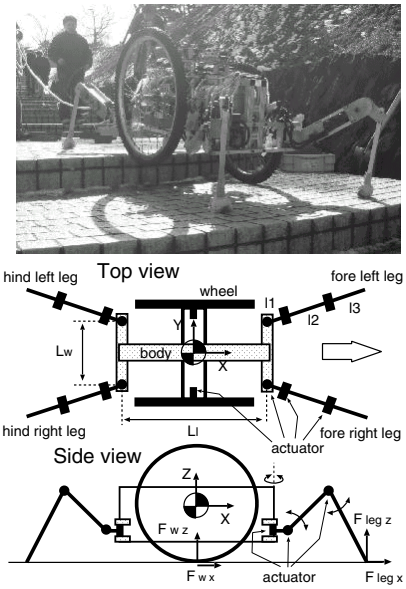

Fig. 1. A leg-wheel robot "Chariot 3".

We proposed 3 gait strategies for rough terrain [3], focusing on terrain with steps 0.1-0.2 m high, and discuss robot control and movement.

Unlike the gait strategy Ohmichi et al. proposed for similar leg-wheel robots [4], which did not target unknown rough terrain, we target such terrain for leg-wheel robots.

Conventional 4- and 6-leg robots traverse rough terrain using force control based on precision force information from the legs [5–9]. We propose movement control for unknown rough terrain using internal sensors alone, i.e., angle sensor of each joint and positioning (pitch and roll). We did not used external sensors because they are less accurate in natural environments such as slopes, steps, weedy or muddy land, or snow involving concomitant errors due to noise and other factors. Our research policy holds that, for practical application, robots traversing unknown rough terrain should move based on information from internal sensors alone. External sensors should be used to further enhance the capability of traversing unknown terrain based on information from internal sensors alone.

1. This paper is the full translation from the transactions of JSME Vol.72, No.721.

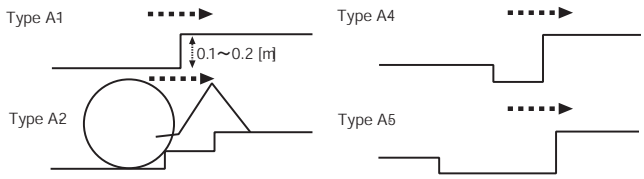

Fig. 2. Targeted rough terrain of a step-up gait.

2. Step-Up Gait

Figure 2 shows our targeted terrain. Type A-1 is a single ascending step 0.1-0.2 m high. Type A-2 is a double step with the middle located between front leg contacts and wheel contacts. Type A-4 and A-5 steps have grooves in the middle. Types A-4 and A-5 differ in whether the wheel drops into the groove [3]. We detail cases in Section 5 in which the robot moves toward a step diagonally, step heights differ laterally, and ascending steps are slanted.

We targeted a gait where the robot is supported by all 4 legs and wheels when raising itself to ascend steps, at which time it is desirable for the wheels to continuously contact the ground and support the robot to ensure stability, energy saving, distributed drive force, and loads. Because topography is difficult to detect precisely and possible topography deviations from the actual, the wheels will not invariably contact the ground, requiring the robot ensure a static stability margin with the legs alone. Although the static stability margin can be ensured using only 3 legs, we used 4-leg support to balance the robot's ability to respond to external longitudinal and lateral disturbance. we call the gait based on this support an all-leg-support gait.

Since we use the all-leg-support gait to traverse rough terrain (**Fig. 3**), we exclude large steps in which the all-leg-support gait cannot raise the robot in a single movement, meaning the robot cannot cope with steps requiring more than one stride width of 0.35 m, which is wide enough to let the robot traverse uneven terrain within 0.2 m high because the stride required to traverse a 0.2 m step is 0.297 m.

For regular rough terrain, the robot is driven by basic movement control [1] using a trot [2] for leg control, also called the "normal" gait. When wheels contact an ascending step using the normal gait, the robot stops moving to detect the start of the ascending step using a method based on wheel angular deviation, detailed later (**Fig. 3(b)**).

Upon detecting the start of a step, the robot locations its legs (preparatory leg repositioning) to ready for the all-leg-support gait, placing all legs in their start locations within their workspaces to maximize gait movement distance (**Figs. 3(c)**, **(d)**). The robot estimates step height by leg positioning and robot inclination after leg repositioning (**Fig. 3(e)**), then raises itself using the all-leg-support gait to reach the estimated height (**Fig. 3(f)**).

When legs have reached movable limits, the all-leg-support gait is completed (**Fig. 3(g)**) and the robot places its legs back in place for the normal gait (end leg replacement) (**Fig. 3(h)**). When the first 2 legs have finished leg repositioning, the robot will initiates the normal gait (**Figs. 3(i)-(l)**).

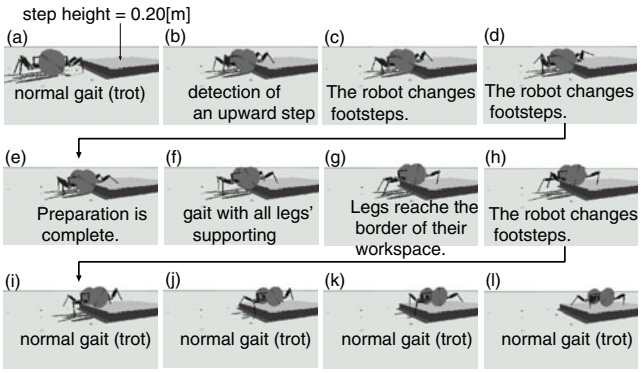

Fig. 3. Step-up gait.

3. Step-Up Gait Control

The sections that follow detail step-up gait control.

3.1. Detection of Step-Up Start Location

When encountering an ascending step, the robot stops moving because it cannot raise itself in the normal gait (**Fig. 3(b)**). Monitoring wheel angular deviation δ_{wi} from the target angle, the robot detect the ascending step start location. δ_{wi} of wheel i is expressed by Eq. (1) using target wheel angle $\theta_{\mathrm{wd}i}$ and current wheel angle θ_{wi} for wheel i.

$$\delta_{wi} = \theta_{\mathrm{wd}i} - \theta_{wi} \quad \ldots\ldots\ldots\ldots\ldots (1)$$

When the smaller of the left and right wheel angles exceeds threshold $\Delta_{w\min}$, the robot detects it as the start location of the ascending step.

$$\min(\delta_{wi}) > \Delta_{w\min} \quad (i = 1,2) \quad \ldots\ldots\ldots (2)$$

We use the smaller angle because, during the normal gait, deviations in the left and right wheels vary with the terrain condition. Using a large angle may cause the threshold to be exceeded even if the robot can traverse terrain using the normal gait. Cases in which the smaller angle exceeds the threshold were those in which the robot was almost unable to move forward.

We decided that an obstacle would be detected when over 80% of time series data was outside of the threshold for 0.45 s to avoid erroneous detection. We did not use single data from a processing cycle because it could increase detection error. Values were determined experimentally.

For threshold $\Delta_{w\min}$, we apply different data depending on the case, as follows:

Regular rough terrain (Case 1): While traversing regular rough terrain, the gait for large rough terrain should not be activated while the normal gait can move the robot. Monitoring H_e (explained later), if it is determined to be regular rough terrain

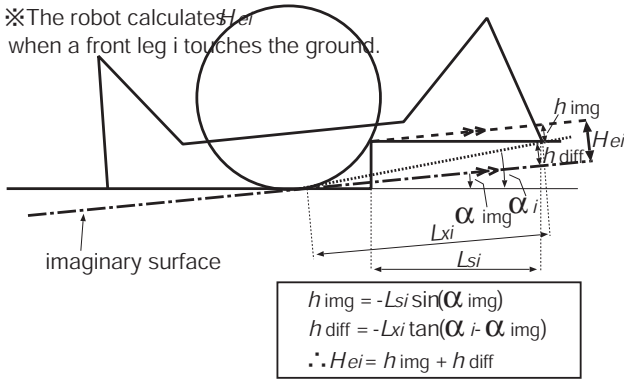

Fig. 4. Estimated step height.

$(\max(H_{ei}) < 0.1\ (i = 1,2))$, the robot applies a larger threshold ($\Delta_{w\min} = 18^\circ$) than for case 2.

The value was determined experimentally on many rough surfaces to keep steps under 0.1 m high from being detected too easily.

Large rough terrain (Case 2): The robot must detect the start of ascending steps promptly in large rough terrain, so we used a smaller threshold ($\Delta_{w\min} = 8^\circ$) for large rough terrain ($\max(H_{ei}) \geq 0.1\ (i = 1,2)$) than for regular rough terrain. This enabled the robot to detect a step 0.06 m high.

When the robot stops, it cannot determine whether an obstacle is an ascending step or a protrusion, which requires the step-over gait [3] instead the step-up gait. The robot selects one based on estimated height H_{ei} (explained later) when it completes preparatory leg repositioning and obtains height (H_{ei}). We determined experimentally that the step-up gait would be selected if either the left or right leg meets $H_{ei} \geq 0.05$ m.

3.2. Step Height Estimation

3.2.1. Estimated Step Height for Leg *i*

In the normal gait, the pitch angle of the robot is adjusted parallel to an imaginary surface [1] obtained from contact locations of the front and back legs and wheels with the ground to provide sufficient leg workspace for all legs to be included in swing phases. To provide movement seamless with the normal gait, the step-up gait takes the robot pitch angle parallel to the imaginary surface. The step height is expressed for the imaginary surface (**Fig. 4**).

Estimated height H_{ei} of leg i can be divided into h_{diff}, attributable to the difference from the imaginary surface, and h_{img}, attributable to the imaginary inclination (the slope of the imaginary surface) (**Fig. 4**). Note that we exclude slanted steps so the step is assumed to be horizontal. The height is estimated from information obtained from the front legs.

Height difference h_{diff} between the leg contact height and imaginary surface is expressed by Eq. (3) using L_{xi} for the location of the front leg in the direction of X in robot coordinates, α_i for the imaginary inclination formed by the front leg, and α_{img} for the imaginary inclination of the robot.

$$h_{\text{diff}} = -L_{xi}\tan(\alpha_i - \alpha_{\text{img}}) \quad \ldots\ldots\ldots \quad (3)$$

where a plus sign (+) represents ascending steps and a minus sign (−) descending steps.

Estimated height h_{img} attributable to the imaginary inclination of the robot is expressed by Eq. (4) using L_{si}, the distance between leg and wheel contacts.

$$h_{\text{img}} = -L_{si}\sin\alpha_{\text{img}} \quad \ldots\ldots\ldots\ldots \quad (4)$$

We approximated L_{si} using L_{xi} subtracted by the wheel radius. The error in this approximation is 0.005 m at most for a step of 0.1 m, which is the smallest height to be traversed by the step-up gait and gives the maximum error.

Using these values, estimated height H_{ei} from the front leg is expressed by Eq. (5). The estimation is calculated when front leg i switches from swing to support phase.

$$H_{ei} = h_{\text{diff}} + h_{\text{img}} \quad \ldots\ldots\ldots\ldots \quad (5)$$

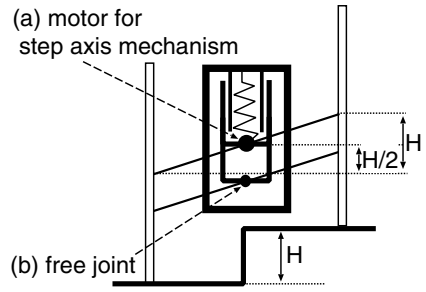

Fig. 5. Height of robot for an uneven step.

3.2.2. Measures for Steps with Laterally Differing Heights

In cases in which the step height differs laterally (on left and right sides), the height to which the robot must be raised is the average of left and right heights (**Fig. 5**). We defined estimated height H_e for the robot to be raised as the average of estimated heights obtained from left and right front legs as follows:

$$H_e = (H_{e\text{fl}} + H_{e\text{fr}}) = 2 \quad \ldots\ldots\ldots\ldots \quad (6)$$

where $H_{e\text{fl}}$ represents the estimated height of the left front leg and $H_{e\text{fr}}$ represents that of the right front leg.

3.3. All-Leg-Support Gait Control

In the all-leg-support gait following preparatory leg repositioning, the robot is supported by its 4 legs and 2 wheels to raise it onto the step.

The gait starts with all legs replaced at the start locations in their workspaces and ends with the legs reaching their movable limits after the robot is raised by the legs and wheels. The all-leg-support gait advances the robot a distance equal to one stride width.

3.3.1. Wheel Control

In movement during the all-leg-support gait (**Fig. 6**), wheels are controlled to turn around point C to keep continuous contact with the assumed surface (**Fig. 6**). We assumed not a slanted step but a step with right angles (**Fig. 6**) because, if we assume slanted step surfaces, steeper step may interfere with the robot.

The imaginary surface considered for one stride at the beginning of the all-leg-support gait passes through points A-D (**Fig. 6**). The robot is controlled so that its pitch angle becomes parallel to the imaginary surface and we assume the robot moves forward parallel to this imaginary surface. The pitch angle is made to the imaginary surface to provide a larger movable range for the front and back legs both in support and swing phases, as in the normal gait [1]. Rotation angle dW_{di} of wheel i for a very short time is expressed by Eq. (7) using dP_{xd} for the target distance change for a very short time in the direction of the X axis of robot coordinates, r for the wheel radius, and θ assigned as in **Fig. 6**. Proportional derivative (PD) control is used to follow the target angles of the wheel.

$$\begin{cases} dW_{di} = dP_{\mathrm{xd}}/(r\cos\theta) & \text{((a) while going up a step)} \\ dW_{di} = dP_{\mathrm{xd}}/r & \text{((b) after going up the step)} \end{cases} \quad \ldots\ldots\ldots\ldots\ldots (7)$$

where θ_s represents the angle between a line segment from the wheel center to point C and a line segment from point C perpendicular to the imaginary surface at the beginning of the all-leg-support gait. The value of dP_{xd} is given as a command and H_e is the estimated height. Other values are obtained geometrically (**Fig. 6**).

As the robot moves toward point D, imaginary and actual surfaces deviate, although 0.003 m at most with a step of 0.1 m in which distance CD becomes maximum, thus giving maximum deviation. Error is acceptable because it is absorbed by leg compliance and wheel suspension.

3.3.2. Leg Control

Leg trajectories are determined geometrically in relation to the robot location (P_{xd}, P_{zd}) as in the case of the wheels.

To raise the robot, the legs must be pushed down. The trajectory of Leg i is obtained from **Fig. 6** as follows:

$$\begin{cases} dP_{\mathrm{zd}i} = -dP_{\mathrm{zd}} & \text{((a) while going up a step)} \\ dP_{\mathrm{zd}i} = 0 & \text{((b) after going up the step)} \end{cases} \quad (8)$$

where dP_{zd} represents the target distance change of the robot for a very short time in the direction of the Z axis of robot coordinates and $dP_{\mathrm{zd}i}$ represents that of leg i.

The leg location in the direction of X and Y in robot coordinates is determined by a gait algorithm proposed previously [2].

In addition to Eq. (8), since legs contact the ground discretely, we require an initial value for target leg contact locations. To absorb disturbances from terrain surfaces by leg compliance as in the normal gait, the targeted leg height when switching from swing to support phases is assigned to be lower than the actual height by Δ_s, the basic setting [1]. Compliance is set as in the normal gait [1] and leg trajectory is adjusted at the same timing as in the normal gait so that the robot pitch angle remains parallel to the imaginary surface.

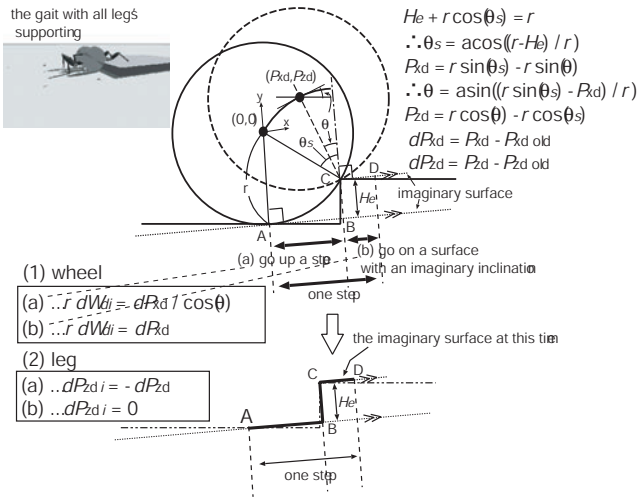

Fig. 6. Wheel and leg control for a gait with all leg supporting.

3.3.3. Step Axis Control

As in the normal gait [1], feedback control is implemented by Eq. (9) based on sky-hook damper theory so that targeted robot roll angle $\theta_{\mathrm{d}r}$ becomes 0 for better stability. The robot roll angle is controlled by the motor on a step axis (**Fig. 5**). T_{θ_r} represents the torque of the motor on the step axis, θ_r the robot roll angle, $\theta_{\mathrm{d}r}$ the target robot roll angle, K_r the angle gain, and D_r angular velocity gain.

$$T_{\theta_r} = -K_r(\theta_r - \theta_{\mathrm{d}r}) - D_r(\dot{\theta}_r - \dot{\theta}_{\mathrm{d}r}) = -K_r\theta_r - D_r\dot{\theta}_r \quad \ldots\ldots\ldots\ldots\ldots (9)$$

Using this control enables the robot to enter a step diagonally, as follows:

When entering a step diagonally, wheels on the left and right sides climb the step at different timing, unlike orthogonal entry. The left wheel, which contacts the step first, climbs the step (**Figs. 7(a)-(c)**) as a result of step axis control that drives the motor to keep the robot roll angle at 0°. Then, the right wheel encounters the step. The robot once stops unable to climb the step in the normal gait and changes the gait to the step-up gait (**Figs. 7(d)-(f)**).

3.3.4. Measures for Over-Estimated Step Height

Since front leg and wheel contacts differ in location, the robot raising height cannot be estimated accurately depending on topography. A double step, for example, step height H_e estimated at the beginning of the all-leg-support gait will be higher than the actual height for the robot to climb first (**Fig. 8**).

Small error in estimated step height H_e is absorbed by leg compliance and wheel suspension, but not error that is large.

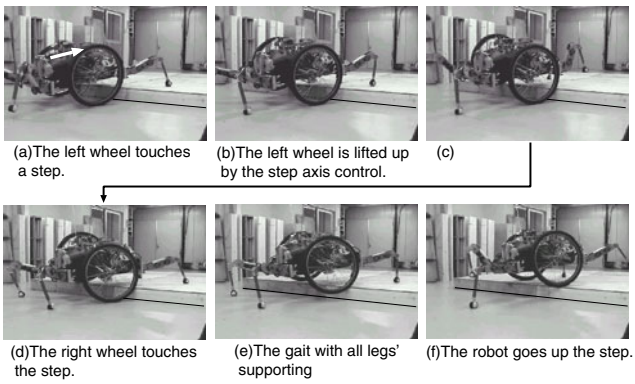

Fig. 7. Effectiveness of step axis control to ascend a step diagonally.

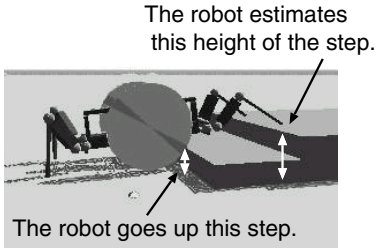

Fig. 8. Terrain with 2 steps.

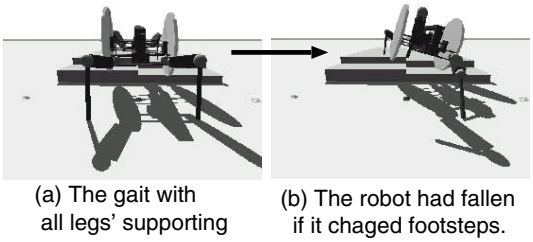

Fig. 9. The robot fell if the step was estimated to be too high.

Here we discuss a case in which the robot is raised too much by over estimation and the wheel cannot contact the ground (**Fig. 9**). While in all-leg-support gait, the robot is supported by all 4 legs, ensuring static stability margin (**Fig. 9(a)**). When the robot lifts legs for leg repositioning at the end of the gait, the robot is supported only by 2 legs, losing stability and possibly falling (**Fig. 9(b)**).

To address this problem, we introduced a leg load sharing monitor algorithm to see if the weight of the robot is sufficiently supported by wheels at the end of the all-leg-support gait so that, if it is not, the robot can be lowered by activating leg relaxation.

The leg load sharing monitor algorithm calculates k_{leg}, the ratio of loads supported by legs using Eq. (10). If it exceeds threshold k_d in duration dt_k at a certain percentage P_k, it activates leg relaxation.

$$k_{\text{leg}} = \frac{\sum_{i=1}^{n}(\delta_{zi}/C_{zi})}{W} \quad \ldots\ldots\ldots\ldots (10)$$

where n represents the number of support legs, δ_i the deviation in actual support leg locations from targets in the direction of the Z axis of robot coordinates ([actual location]-[target location]), C_{zi} the compliance of support leg i in the direction of the Z axis, and W the weight of the robot. k_{leg} shows a portion of the weight supported by the legs. We experimentally assigned $dt_k = 0.45$, $P_k = 0.8$, $k_{\text{d1}} = 0.65$ (for normal gait), and $k_{\text{d2}} = 0.60$ for all-leg-support gait.

Leg relaxation is achieved by raising the target location of the leg – the robot is lowered – until the leg load sharing ratio falls below a certain value.

3.3.5. Measures for Underestimated Step Height

If a protrusion exists between the front leg contacts and wheel contacts, estimated step height H_e is lower than the actual height the robot must climb.

If estimation error is large, the robot cannot climb the step. If the robot determines it cannot do so, it does as follows:

The step climbing decision is made by monitoring the deviation of wheel angles from targets. As deviation increases, the robot determines it cannot climb the step and changes to the step-over gait as detailed elsewhere [3].

4. Simulation and Experiments

We verify in this section that the proposed gait enables robots to traverse the targeted large rough terrain.

Simulation and experiment conditions were as follows: swing leg speed was 0.5 m/s, swing leg lifting height 0.2 m, maximum leg lowering for a swing leg to land 0.4 m, stride width 0.35 m, basic deviation of actual leg locations from targets $\Delta_s = 0.043$ m, stiffness for all legs and for suspension in the direction of the Z axis 7500 N/m, the basic load sharing ratio between legs and wheels 1:1, P and D gains for wheel rotation control 80 Nm/rad and 20 Nm/rad/s, and P and D gains for step axis control 1000 Nm/rad and 100 Nm/rad/s. The gait was a trot [2] and the environment was assumed to be unknown. We used the Open Dynamics Engine (ODE) to dynamically simulate assuming rigid contact between the legs and ground and the wheel and ground. The friction coefficient between the legs and ground was set at 0.4 and that between the wheels and ground at 0.7.

4.1. Type A-1 Terrain

4.1.1. Simulation

Simulation was made with an unknown ascending step 0.20 m high (**Fig. 10(a)**). Results showed successful traversing over an unknown ascending step of 0.20 m (**Fig. 10(b)**) and data (**Figs. 11(a)-(f)**).

Figure 11(a) shows robot target translational velocities. The robot replaced legs in period (1), where velocity $V_{\text{body}} = 0$, and took the all-leg-support gait in period (2) (**Fig. 11(a)**). Small fluctuations in target velocities result from restrictions on velocity commands activated by event-driven control (2). Note that velocity $V_{\text{body}} = 0$ in period (3). This is for leg relaxation activated during a normal gait, where leg load sharing ratio k_{leg} drops after exceeding the threshold at time (6) (**Fig. 11(d)**).

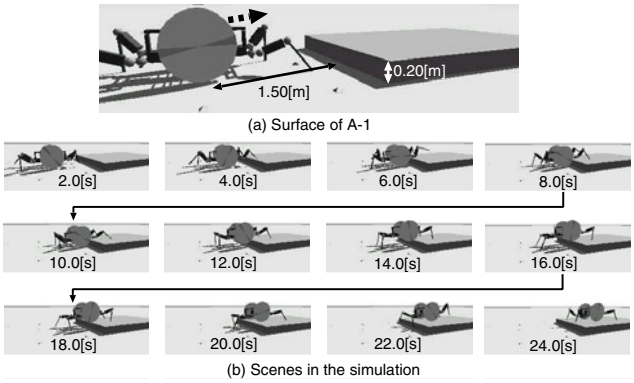

Fig. 10. Simulation of Type A-1 terrain.

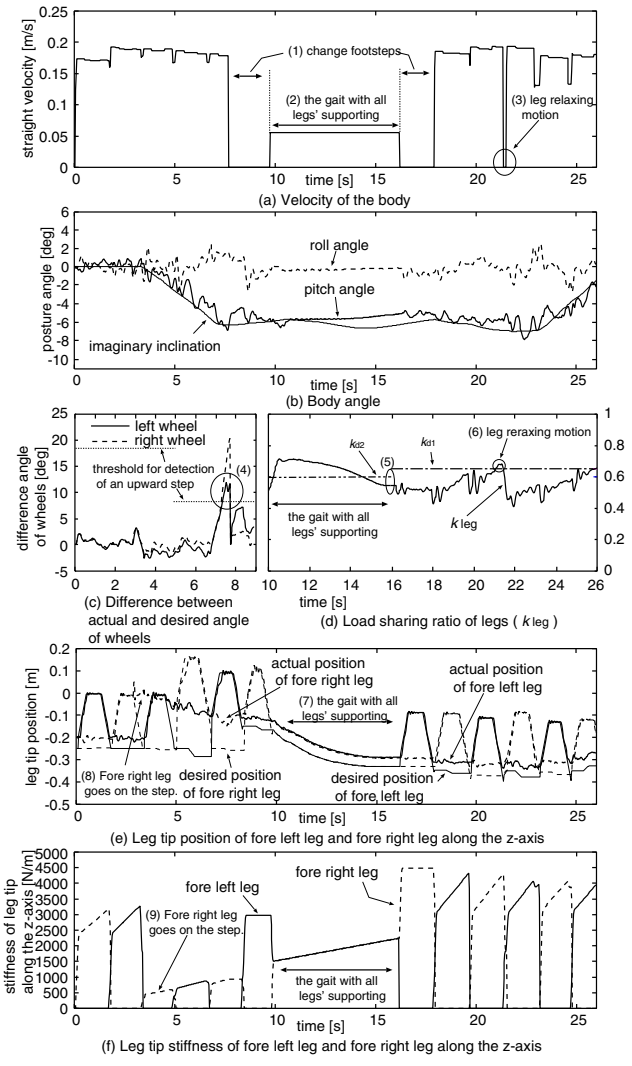

Fig. 11. Simulation data for Type A-1 terrain.

Figure 11(b) shows the transition of robot pitch and roll angles. Note that the robot pitch angle followed the imaginary inclination well and the robot roll angle was kept horizontal.

Figure 11(c) shows deviations in left and right wheel angles from their target angles (wheel angular deviations) during time $t = 0 - 9$ s. The ascending step was detected at time (4) when the smaller angular deviation of the left wheel had exceeded threshold 8° for 80% of 0.45 s (values experimentally determined). After detection, the target wheel angle was reset to the current value, thereby resetting wheel angular deviation to 0.

Figure 11(d) shows leg load sharing ratios k_{leg} during time $t = 10 - 27$ s. The robot compared k_{leg} to threshold $k_{\text{d2}}(= 0.6)$ at time (5) just before the all-leg-support gait was completed to see if it had not raised the robot too much. It did not exceed the threshold, determining not to have raised the robot too much and activating no leg relaxation movement. At time (6) in the normal gait, the leg load sharing monitor functioned at threshold $k_{\text{d1}}(= 0.65)$, causing the robot to stop activating leg relaxation, so k_{leg} dropped to the target value 0.5.

Figure 11(e) shows the target and actual front (left and right) leg locations in the direction of the Z axis in robot coordinates. At time (7) when the all-leg-support gait started, target locations for legs were lowered to raise the robot. Estimated step height H_e was calculated at 0.179 m and target heights were lowered to match it. For reference, theoretical H_e for step height 0.2 m is 0.181 m. The deviation of actual leg locations from targets was attributable to leg compliance and legs were controlled keeping compliance even in the all-leg-support gait. At time (8) where the right front leg landed on the step, the deviation in the leg location increased.

Figure 11(f) shows front leg stiffness in supporting phases. Leg stiffness in swing phases is displayed as 0 for graphs. Leg stiffness decreased on legs in the all-leg-support gait because the robot was supported by all legs. The stiffness of the right front leg decreased at time (9) because the robot adjusted (decreased) stiffness as positional deviation increased at time (8) (**Fig. 11(e)**) so that it would not apply extra force to the legs.

4.1.2. Experiments

Experiments were made with an unknown ascending step having height 0.20 m (**Fig. 12(a)**). Topography was the same as in **Fig. 10**. **Fig. 12(b)** shows results showing traversing over an unknown ascending step of 0.20 m.

Due to space limitation, only robot angle data is shown in **Fig. 12(c)**. Robot angles were about the same as those obtained by simulation. Robot angles in experiments fluctuated more than in simulation, presumably due to joint friction and modeling errors in the robot. The estimated step height was $H_e = 0.174$. We confirmed that other experimental data matched that obtained by simulation.

5. Traverse Experiments on Other Rough Terrain

This section discusses cases in which the robot moves diagonally toward a step, for which step heights differ laterally and where ascending steps are slanted, as well as cases in **Fig. 2**. We confirmed traversal on all terrain by both simulation and experiments. Due to space limitation, we summarize experiments here.

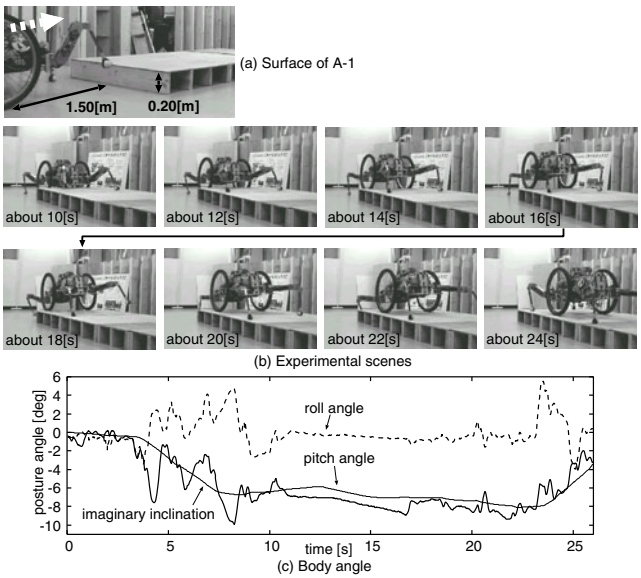

Fig. 12. Experiments for Type A-1 terrain.

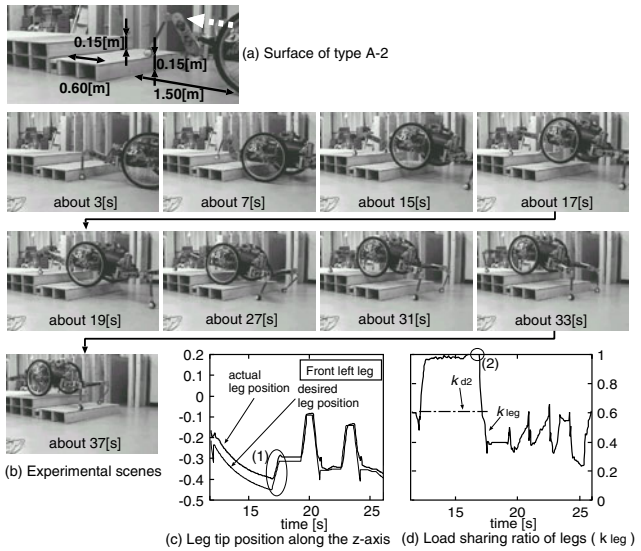

Fig. 13. Type A-2 terrain.

5.1. Type A-2 Terrain

Figure 13(b) shows experimental results with a double step (**Fig. 13(a)**) whose first step is 0.60 m and heights of individual steps is 0.15 m. Estimated heights were 0.230 m for the first step and 0.131 m for the second step. **Fig. 13(c)** shows target and actual locations for the left front leg in the direction of the Z axis in robot coordinates. During the step-up gait for the first step, the front leg landed on the top of the second step, while the robot had to be raised for one step height, causing overestimation in height for robot raising. To offset the difference, the robot was lowered at time (1) by raising the target leg location. **Fig. 13(d)** shows the transition of leg load sharing ratio k_{leg}. When the all-leg-support gait was completed at time (2), k_{leg} was higher than threshold k_{d2}, so the robot lowered itself at time (1) until wheels landed on the first step and the load sharing ratio was reduced

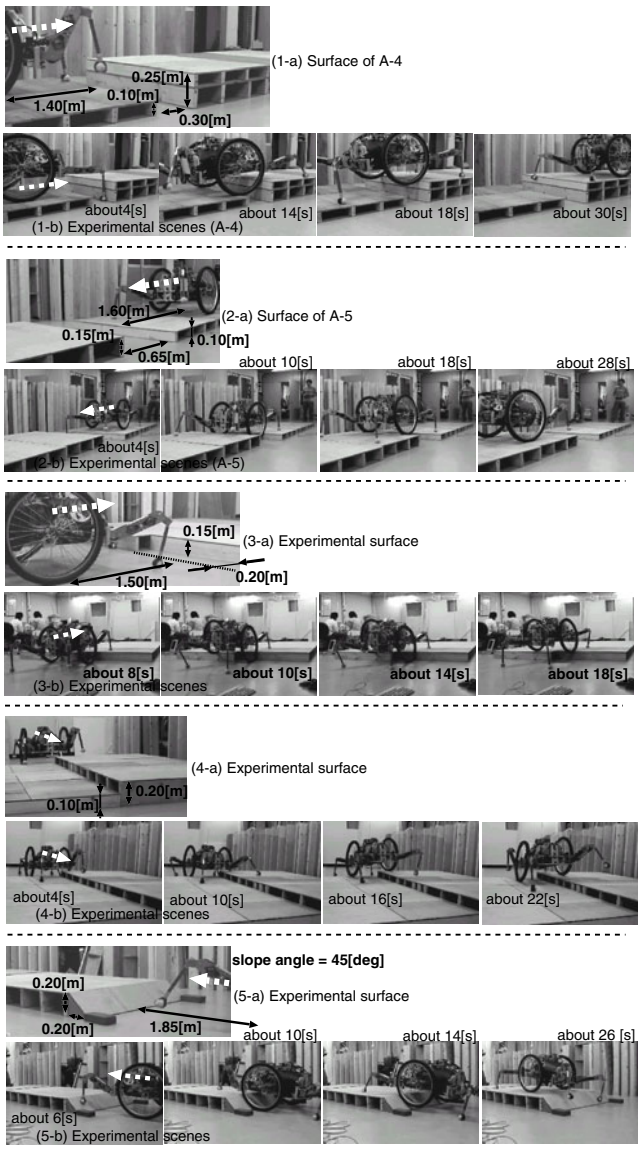

Fig. 14. Other rough terrain.

(**Fig. 13(c)**). The robot thus traversed the step stably.

5.2. Type A-4 Terrain

Figure 14(1-b) shows experimental results with terrain (**Fig. 14(1-a)**) in which a groove with the width of the wheel radius is located before an ascending step. Since wheels were bigger than the groove and did not drop into it, the robot traversed as in the Type A-1 terrain.

5.3. Type A-5 Terrain

Figure 14(2-b) shows results of similar experiments but with a wider groove (**Fig. 14(2-a)**), about the width of the wheel diameter. The wheel dropped into the groove but kept moving to the step in the normal gait and then climbed the step as for Type A-1 terrain.

5.4. Diagonal Entrance to Step

When entering a step diagonally, compared to orthogonally, step starting points for the robot differed between

left and right sides.

To evaluate this, we conducted experiments (**Fig. 14(3-b)**) with a step (**Fig. 14(3-a)**) 0.15 m high having different starting points by 0.2 m between left and right sides. The left wheel climbed the step in the normal gait and then the right wheel contacted the step. It could not climb the step, so the robot changed to the step-up gait.

5.5. Step with Laterally Different Heights

We conducted experiments with a step (**Fig. 14(4-a)**) whose height differed laterally for the robot (**Fig. 14(4-b)**). The robot traversed the step keeping its robot roll angle horizontal using step axis control even though step heights differed on both sides.

5.6. Slanted Ascending Step

We conducted experiments with a slanted ascending step (**Figs. 14(5-a)** and **(5-b)**). The robot traversed the step by absorbing the difference between the assumed and actual topography by compliance. We also confirmed that the robot successfully traversed topography with multiple steps on a long slope by using multiple step-up gaits if the topography provided space for wheels to land surely during leg repositioning.

6. Conclusions

We have proposed control for step-up gait for leg-wheel robots as an adaptive gait for large rough terrain. Traversing was demonstrated by both simulation and experiments on such terrain using the proposed gait. Simulation and experiments for all targeted topography confirmed that the proposed gait enabled the robot to successful traverse terrain (part of results reported due to space limitations).

We will continue studying gaits for such terrain using the remaining two movement strategies, i.e., step-down and step-over, to propose and verify their control, to be reported elsewhere.

References:

[1] S. Nakajima, E. Nakano, and T. Takahashi, "The Motion Control Method for a Leg-wheel Robot on Unexplored Rough Terrains," Journal of the Robotics Society of Japan, Vol.22, No.8, pp. 1082-1092, 2004.

[2] S. Nakajima, E. Nakano, and T. Takahashi, "Trot and Pace Gaits based on the Predictive Event Driven Method for a Leg-wheel Robot," Journal of the Robotics Society of Japan, Vol.22, No.8, pp. 1070-1081, 2004.

[3] S. Nakajima and E. Nakano, "Adaptive Gait for Large Rough Terrain of a Leg-wheel Robot (First Report: Gait Strategy)," Journal of Robotics and Mechatronics, Vol.20, No.5, pp. 801-805, 2008.

[4] T. Ohmichi and T. Ibe, "Development of Vehicle with Legs and Wheels," Journal of the Robotics Society of Japan, Vol.2, No.3, pp. 244-251, 1984.

[5] S. M. Song and K. J. Waldron, "Machines That Walk: The Adaptive Suspension Vehicle," MIT Press, 1989.

[6] K. K. Hartikainen, A. J. Halme, H. Lehtinen, and K. O. Koskinen, "MECANT I:A Six Legged Walking Machine for Research Purposes in Outdoor Environment," Proc. of the 1992 IEEE Int. Conf. on Robotics and Automation, pp. 157-163, 1992.

[7] D. M. Gorinevsky and A. Shneider, "Force Control of Legged Vehicles over Rigid and Soft Surfaces," Int. Journal of Robotics Research, Vol.9, No.2, pp. 4-23, 1990.

[8] J. E. Bares and W. L. Whittaker, "Configuration of Autonomous Walkers for Extreme Terrain," Int. Journal of Robotics Research, Vol.12, No.6, pp. 535-559, 1993.

[9] T. Hori, H. Kobayashi, and K. Inagaki, "Force Control for Hexapod Walking Robot with Torque Observer," Proc. of the Int. Conf. on Intelligent Robots and Systems, pp. 1294-1300, 1994.

Name:
Shuro Nakajima

Affiliation:
Ph.D. (Information Science), Associate Professor, The Department of Advanced Robotics, Chiba Institute of Technology

Qualification:
Professional Engineer (Mechanical Engineering)

Address:
2-17-1 Tsudanuma, Narashino, Chiba 275-0016, Japan

Brief Biographical History:
1997- East Japan Railway Company
2005- Future Robotics Technology Center, Chiba Institute of Technology
2006- The Department of Advanced Robotics, Chiba Institute of Technology

Main Works:
• S. Nakajima, E. Nakano, and T. Takahashi, "Motion Control Technique for Practical Use of a Leg-Wheel Robot on Unknown Outdoor Rough Terrains," Proc. of the Int. Conf. on Intelligent Robots and Systems, Vol.1, pp. 1353-1358, September, 2004.

Membership in Academic Societies:
• Institute of Electrical and Electronics Engineers (IEEE)
• The Japan Society of Mechanical Engineers (JSME)
• The Robotics Society of Japan (RSJ)
• Japan Society of Kansei Engineering (JSKE)
• The The Institution of of Professional Engineers, Japan (IPEJ)

Name:
Eiji Nakano

Affiliation:
Docter of Engineering, Professor, The Department of Advanced Robotics, Chiba Institute of Technology

Address:
2-17-1, Narashino-shi, Chiba 275-0016, Japan

Brief Biographical History:
1970 Graduated, Postgraduate Course of University of Tokyo
1970 Senior Researcher, Mechanical Engineering Laboratory
1987 Professor, Tohoku University
2005 Professor, Chiba Institute of Technology

Main Works:
• E. Nakano, et al, "Leg-Wheel Robot: A Futuristic Mobile Platform for Forestry Industry," 1993 IEEE/Tsukuba Industrial Workshop on Advanced Robotics, 1993.

Membership in Academic Societies:
• Robotics Society of Japan (RSJ)
• Japan Society of Mechanical Engineers (JSME)
• Society of Instrument and Control Engineers (SICE)
• Society of Biomechanism (SOBIM)